Available online at www.sciencedirect.com
ScienceDirect
Journal of the European Ceramic Society 29 (2009) 2747–2756
www.elsevier.com/locate/jeurceramsoc

Relationships between microstructure, mechanical and dielectric properties of different alumina materials

L. Haddour [a], N. Mesrati [a], D. Goeuriot [b], D. Tréheux [c,*]

[a] *Laboratoire Science et Génie des matériaux, Ecole Nationale Polytechnique, B.P 182, 10 Avenue Hassen Badi, El Harrach 16200 Alger, Algeria*
[b] *Départment Mécanique, Procédés d'Elaboration UMR-CNRS 5146, ENS Mines de Saint-Etienne 158, cours Fauriel 42023 Saint-Etienne Cedex 2, France*
[c] *Laboratoire de Tribologie et Dynamique des Systèmes, UMR CNRS 5513, Ecole Centrale de Lyon, 69134 Ecully cedex, France*

Received 2 December 2008; received in revised form 27 February 2009; accepted 13 March 2009
Available online 6 May 2009

Abstract

Different alumina materials were elaborated in order to vary microstructural parameters (grain size, densification, porosity, inter-granular phase). These ceramic materials were then characterized from the mechanical point of view (hardness, toughness, friction and wear) and dielectric breakdown. The comparison of these various results shows that, for all these properties, the grain size and also, the nature of the secondary phases and the microstructural parameters were the most significant.

Moreover, from the tribological point of view, the dielectric characteristic of materials (breakdown strength) has a fundamental role in the creation of agglomerated wear debris ("third body") and its properties: a finely agglomerated third body will be obtained for high breakdown strength. Such third body will be able to protect the substrate and thus to reduce later wear. In the same logic a correspondence between breakdown strength and toughness was established, thus confirming the existence of mechanical–electrical correlation for non-conductive materials.

Keywords: Al_2O_3; Microstructure final; Toughness and toughening; Reinforcement; Wear resistance; Breakdown

1. Introduction

Ceramics are potentially interesting for industrial applications under severe conditions of service. Their wear resistance and their high melting point make them attractive. However, their brittleness makes their use problematic, due to a possible lack of reliability related to their fabrication, inducing structural defects such as porosity, grain size and inter-granular phases. The effect of these microstructural parameters on the mechanical properties of alumina materials was studied for a long time, sometimes with contradictory results. For example the fracture strength slightly decreases as the grain size D, then falls brutally beyond 120 μm.[1] The fracture energy γ (or toughness) decreases as D increases, but other authors note the reverse. In fact,[2] it seems that γ increases as D for $D < 100$ μm, taking into account the development of microcracks,[3,4] then decreases for $D > 100$ μm because of the residual stresses.[5] Hardness would increase slightly[6] as the grain size by an effect of inter-granular embrittlement related to the alumina anisotropy.[7] A coupled effect between grain size and porosity is often announced,[8,9] the porosity effect being more obvious for the low grain sizes. Let us note however that these results are often obtained on a broad range of grain sizes and do not take account of the nature of the inter-granular secondary phases. The zirconia effect on the mechanical properties of alumina is widely known by its toughening effect by microcracking and/or phase transformation,[10,11] but the coupled effect of the other characteristics of alumina is little studied.

The effect on dielectric breakdown is less studied but it is complex. The effect of the grain size [12,13] and porosity[12–14] is obvious but it has been easier to observe grain boundary influence according to impurities contents and impurities type.[12,13,15] It has been determined that the presence of a secondary phase has a strong impact on breakdown and the presence of fine inter-granular zirconia can improve alumina breakdown strength.[12]

Wear of ceramics, analysed using the classical mechanical properties (in particular hardness and toughness) is reported through several experimental studies[16–21] connected with such

* Corresponding author. Tel.: +33 0 4 72 18 64 33.
E-mail address: daniel.treheux@ec-lyon.fr (D. Tréheux).

0955-2219/$ – see front matter © 2009 Elsevier Ltd. All rights reserved.
doi:10.1016/j.jeurceramsoc.2009.03.022

Table 1
Composition and characteristics of alumina ceramic materials (wt %).

N°	% Al_2O_3	% SiO_2	% MgO	% CaO	% ZrO_2	%Additives (except zirconia)	*D*%	$D_{50\ (\mu m)}$	$D_{por\ (\mu m)}$
A	93.26	4.93	1.81	0.00	0.00	6.74	95.60	2.14	4.89
B	92.83	3.86	1.27	2.04	0.00	5.13	95.70	1.85	4.16
D	86.96	6.00	1.46	0.96	4.61	8.42	93.40	2.43	9.87
E	89.15	5.13	0.99	0.00	4.73	6.12	89.40	2.15	5.83
F	88.76	4.09	0.48	1.96	4.71	6.53	95.40	3.28	5.15
G	87.87	5.21	1.25	0.98	4.69	7.44	95.80	2.27	5.04
H	90.12	4.30	0.76	0.00	4.81	5.06	93.50	3.10	4.76
I	89.72	3.25	0.24	2.00	4.79	5.49	95.40	2.96	5.77

D%: Densification, measured starting from the composition of initials minerals, D_{50}: average grain size measured by the intercept method on 500 grains, after polishing and etching. D_{por}: diameter of pores measured starting from fracture topography to avoid the artefacts related to polishing (pull out of grains).

parameters as the grain size or the porosity. On the other hand, phenomena, such as dielectric breakdown, transition mode from mild wear to severe wear,[18] increase in the number of dislocations in brittle ceramics during indentation test[22] or before breakdown,[23] remained misunderstood until taking into account of the polarization property of non-conductive materials.[12,13,17,23–25]

Indeed, all the materials, in particular the insulators, during contacts are subject to the developing of electrical charges and the appearance of electric fields.[26–28] In fact**,** during friction, excess electric charges are injected into an insulator. These charges can diffuse in the material or can be trapped at sites which, in ceramics, correspond to local or longer range structural defects (point defects, grain boundaries, dislocation). Consequently, polarization energy (5 eV/trapped charge) is stored in the material and increases in friction coefficient are observed.[26] After a given time, polarization energy can be catastrophically released inducing severe wear.[17] In the case of alumina, the grain boundaries are privileged sites of trapping and consequently of brutal release of the polarization energy. This led to the inter-granular character of the wear of polycrystalline alumina by "breakdown" of the grain boundaries.[17] Besides, a certain analogy between breakdown[23] and wear[29] is noted**:** in both cases creation of dislocations occurs before the appearance of the catastrophic effect (breakdown or wear), corresponding to the release of the polarization energy in the zones where strong localization of trapped charges appear, i.e. very often at the grain boundaries.[17]

The aim of this work consists in deducing a correlation, resolutely original, between electrical breakdown and mechanical or tribological properties. In this way, these properties being connected, as shown previously, individually to microstructure, we studied, first of all, the role of the microstructure of selected polycrystalline alumina materials on different properties of use (hardness, toughness, friction, and breakdown).

2. Experimental procedure

2.1. Materials

The alumina ceramics, were fabricated by the Ecole Nationale Supérieure des Mines de Saint-Etienne. The starting material was alumina powder issued from the Bayer process ($d_{50} = 1.5\ \mu m$) and different minerals that leads to oxides additives (SiO_2, MgO, CaO, ZrO_2). The powders were prepared according to procedures using aqueous dispersion, adding of organic binders (2% PVA: polyvinyl alcohol and −1% PEG: polyethylene glycol), spray drying and cold uniaxial pressing (30 MPa pressure). The samples are discs, approximately 2 cm diameter and 3 mm thickness. Materials were liquid phase sintered in air, between 1500 and 1600 °C for 1–2 h, in order to obtain various microstructures. The compositions of alumina ceramics, along with other characteristics, are summarized in Table 1. Thus, the samples have variable densifications, relatively weak ($D\% < 95.7$) for better highlighting the relation grain size porosity, often announced in the literature.[8,9] This porosity is closed as the breakdown tests, performed in oil, will prove it. We notice the presence of zirconia too, with nearly the same content for six nuances. The addition of zirconia was selected to highlight its role on the other intrinsic microstructural parameters of alumina. The starting zirconia powders are monoclinic. We checked, by diffractionX, that the zirconia remained monoclinic after sintering, in spite of the possible reactions with the additives. The nature of the inter-granular phases is always difficult to know. However, we determined by X-rays diffraction, on three nuances, the nature of the crystalline phases present in the grain boundaries, associated with the vitreous phase (Table 2).

2.2. Testing procedures

Before all characterizations, the samples were polished, using SiC abrasive papers, and finally diamond pastes (6, 3 and 1 μm). Subsequently, the samples are put in an acetone bath for ultrasonic cleaning. The Vickers's hardness was measured under an applied load of 30 N using ZWICK apparatus.

The fracture toughness values K_{IC} were determined by the indentation method, under applied load of 100 N for 30 s. The

Table 2
Nature of the secondary phases present in studied ceramics.

Ceramics	Secondary crystalline phases
B	Spinel, corundum, anorthite,
F	corundum, Spinel, anorthite, cordierite, gehlenite.
H	Spinel, corundum, cordierite.

fracture toughness K_{IC} is calculated using Liang's relationship[30]

$$K_{IC} = \frac{H_V a^{1/2}}{\alpha}\left(\frac{E\Phi}{H_V}\right)^{0.4}\left(\frac{c}{a}\right)^{c/18a-1.51} \quad (1)$$

$$\alpha = 14\left[1 - 8\frac{(4\nu - 0.5)^4}{1-\nu}\right] \quad (2)$$

With: E = Young's modulus (390 GPa); ν = Poisson's ratio (0.27); $\Phi = 3$ for alumina; H_V = Vicker's microhardness. $2a$ diagonal of indentation; $2c$ total length of cracking.

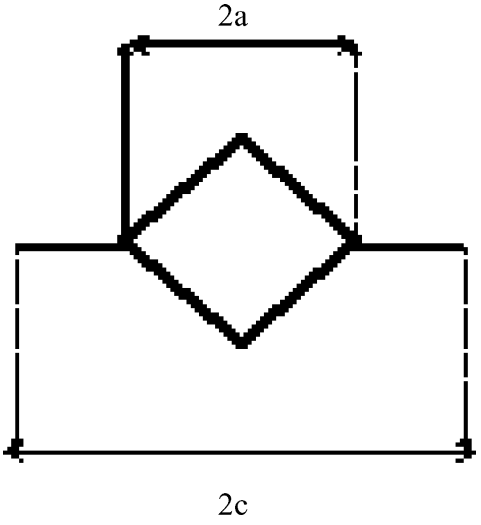

The friction tests were performed at room temperature using a pin on disk reciprocating tribometer.[26] The reciprocating motion is ensured by a crank-connecting rod system. The amplitude of the movement was 5 mm. The pin is a ball (12 mm diameter—99.5% alumina) and the dimensions of the plane are 20 mm × 15 mm × 3 mm. The normal load of 1 or 6 daN is applied directly to the pin. The friction coefficient μ was continuously recorded as a function of the number of cycles via a computer. The wear volumes of different ceramics were evaluated by measuring the depth and the width of the worn track using a profilometer. To determine the wear mechanisms and surface damaging processes, the worn surfaces were examined using a scanning electron microscope (SEM).

To measure the breakdown strength, the experimental device includes a generator delivering an 50 Hz alternating current.[12,13] The sample was placed between the two electrodes of the generator which are immersed in a medium (NITRO10GB-NYNAS transformer oil) whose resistance to dielectric breakdown was higher than that of the tested sample. Breakdown strength (kV/mm) is the ratio of the generator breakdown voltage V_c (in kV) to the thickness e_p of the sample (in mm):

$$E_c^{e_p} = \frac{V_c}{e_p} \quad \left(\frac{\text{kv}}{\text{mm}}\right) \quad (3)$$

Breakdown strength varies with the thickness of the sample. It was thus necessary to make the following correction to the value of $E_c{}^{e_p}$, so that it reflected the resistance to the breakdown of a 3 mm thickness as a standard of comparison[10]:

$$E_c = E_c^{e_p}\sqrt{\frac{e_p}{3}} \quad \left(\frac{\text{kv}}{\text{mm}}\right) \quad (4)$$

The average values as well as the standard deviations were given for a minimum batch of 15 experimental values.

3. Experimental results

3.1. Microstructural observations

The SEM microstructural observations carried out on the samples before friction (Fig. 1), in general, show the same aspect

Table 3
Values of various measured characteristics of alumina.

Ceramics	H_{V_3} GPa	K_{IC} MPa m$^{1/2}$	V_1 10^{-3} mm^3 (100 cycles)	V_2 10^{-3} mm^3 (400 cycles)	Time before stabilization of μ (number of cycles)
A	12.6	6.3 ± 0.7	2.41	39.98	25
B	9.3	7.4 ± 0.5	1.65	12.91	10
D	9.4	8.4 ± 0.6	11.9	85.93	10
E	9.6	7.4 ± 0.4	0.62	34.79	25
F	11.5	9.96 ± 0.3	4.24	12.09	12
G	9.6	8.7 ± 0.8	1.80	69.5	25
H	11.4	8.5 ± 0.7	3.40	74.19	8
I	10.7	9.6 ± 0.8	3.17	73.69	5

Ceramics	E_c kV/mm	Standard deviation
A	14.1	0.4
B	13.9	0.8
D	14.0	0.7
E	13.0	1.5
F	14.9	0.7
G	13.5	0.5
H	14.4	0.4
I	13.3	0.7

H_V, microhardness; K_{IC}, toughness; V_1, wear volume after 100 friction cycles; V_2, wear volume after 400 friction cycles, Time before stabilization of friction coefficient μ; E_C: Breakdown strength as well as the standard deviation.

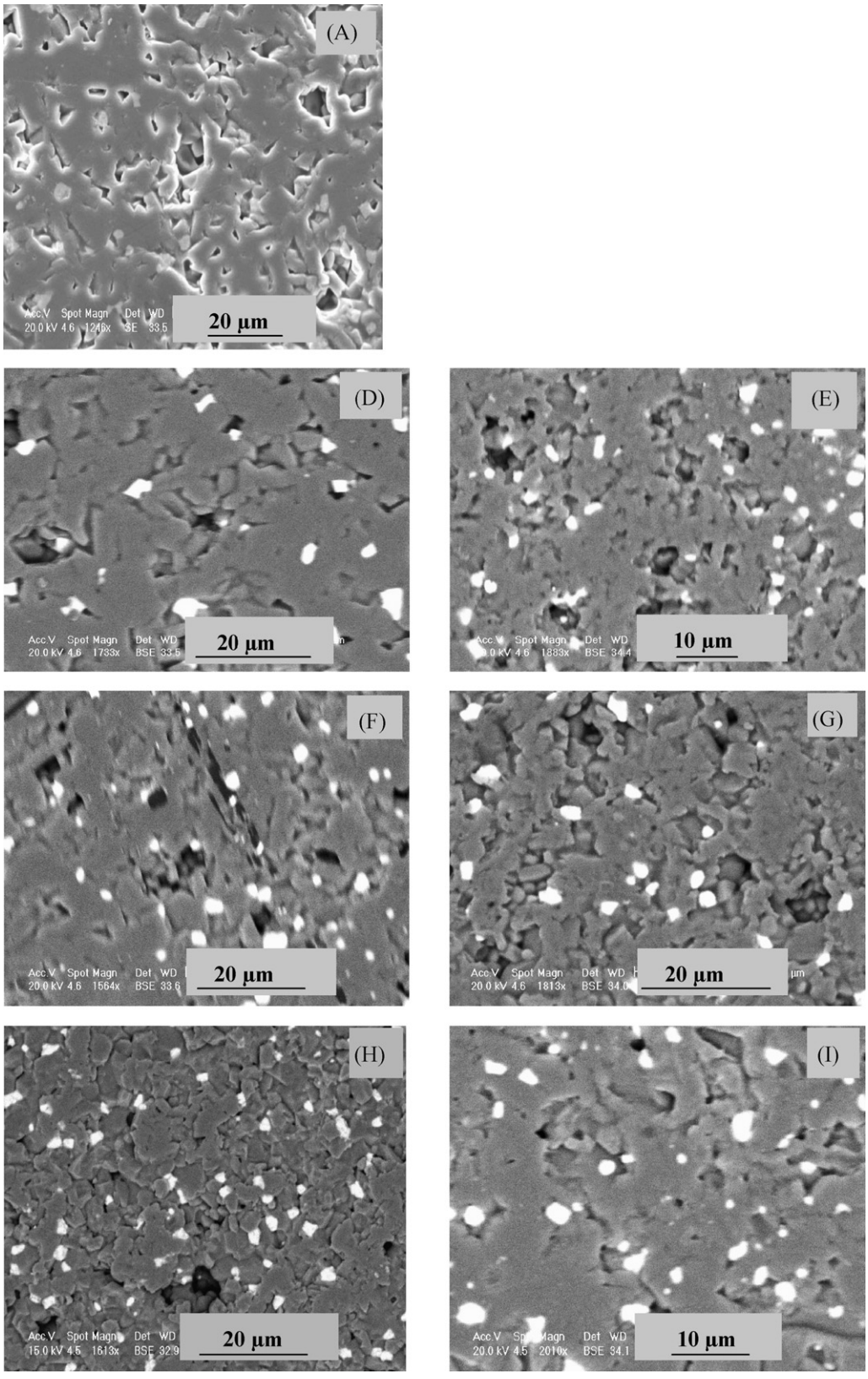

Fig. 1. Backscattered electron image, before friction, of various ceramics materials. Zirconia grains appear in white.

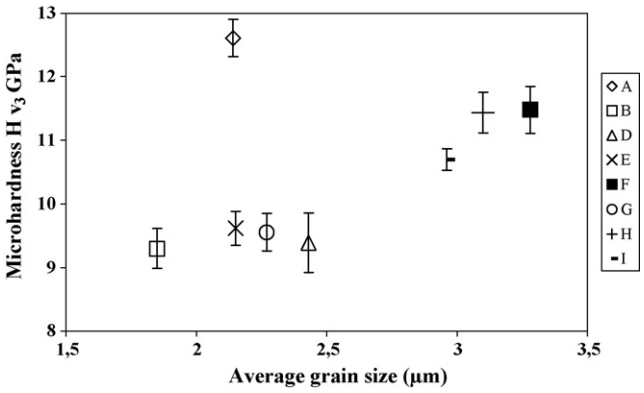

Fig. 2. Evolution of the microhardness vs. average grain size.

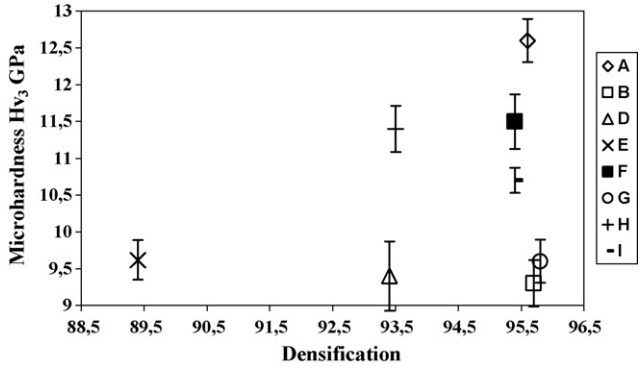

Fig. 3. Evolution of the microhardness vs. densification *D*%.

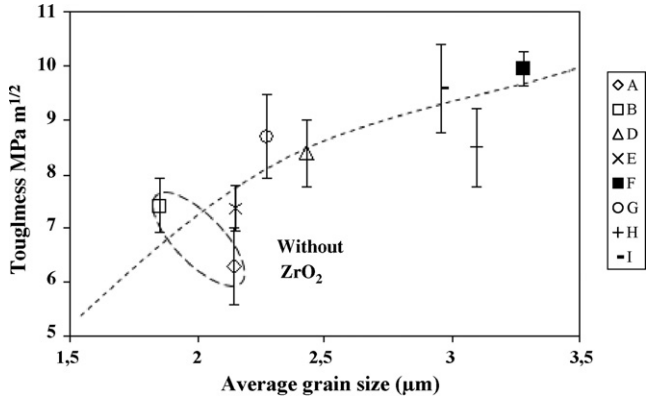

Fig. 4. Evolution of the toughness vs. grain size.

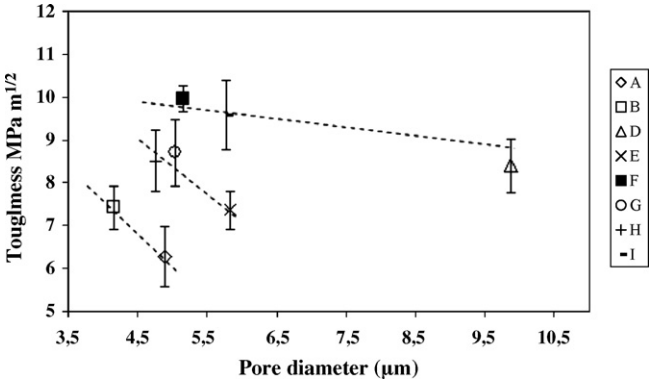

Fig. 5. Evolution of toughness vs. diameter of pores.

for all the alumina ceramics. The porosities present on the surface may be due to the manufacturing process, but they are also due to polishing preparation. Zirconium oxide grains, appearing in white in retrodiffused mode, are homogeneously distributed.

3.2. Mechanical characterizations

Mechanical and dielectric characteristics, detailed after, are summarized in Table 3.

3.2.1. Microhardness

The values of microhardness (average of 6 indentations) are noted in Table 3.

Fig. 2 illustrates the evolution of hardness as a function of average grain size. It is obvious that microhardness increases with increase in average grain diameter in particular beyond 2.5 μm, independently of densification. This result is in agreement with literature[7] and can be attributed to an embrittlement

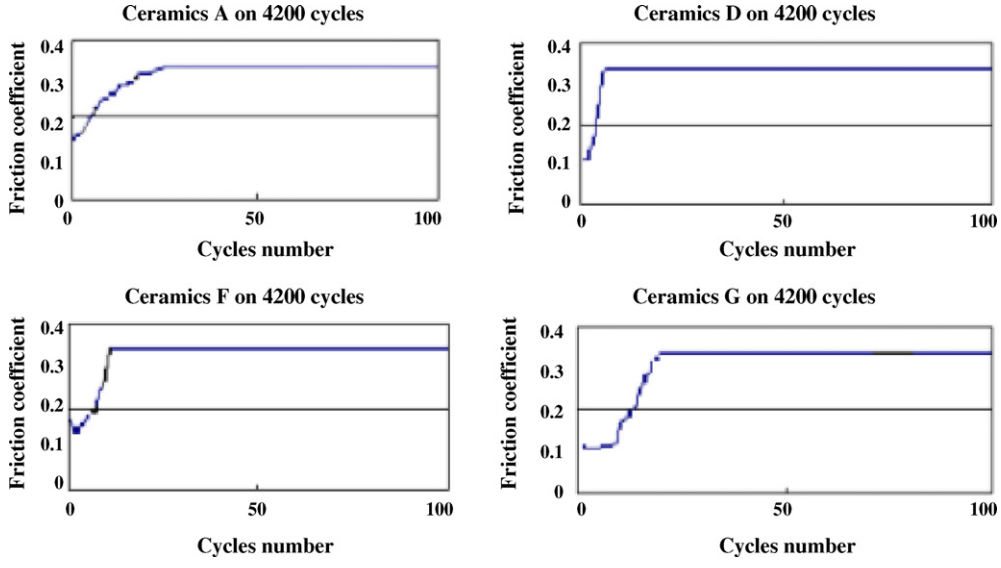

Fig. 6. Some examples of the evolution of the friction coefficient vs. number of cycles.

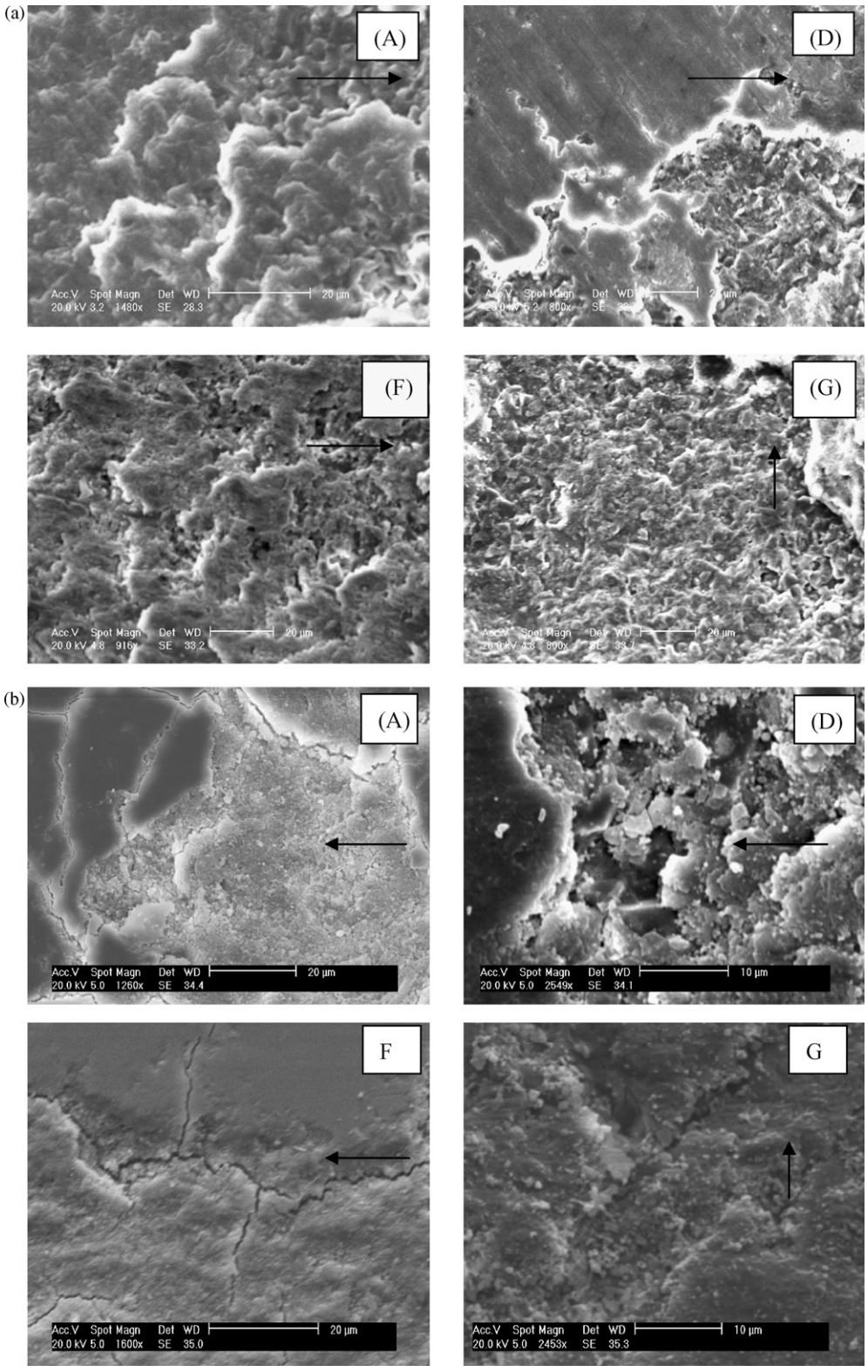

Fig. 7. Friction tracks for a load of 1 daN (SEM).Arrows indicate the friction direction. (a) After 100 cycles and (b) after 400 cycles.

effect induced by grain boundaries, and the tendency of materials with fine grains to become isotropically deformed. A significant hardness increase is noted for ceramics A which moves clearly away from the curve. This alumina contains neither CaO nor ZrO_2.

Fig. 3 shows that, for the low grain sizes (around 2 μm; ceramics E, D, B and G) the microhardness (close to 9.5 GPa) is independent of densification. The same conclusion can be made for the grain sizes close to 3–3.2 μm (ceramics I, H, F), with a hardness near 11 GPa. The hardening effect, beyond a

grain size higher than approximately 2.5 μm, independently of densification, is confirmed.

3.2.2. Fracture toughness

The results (30 s indentation time, average of 15 indentations) are summarized in Table 3. The evolution of fracture toughness with the average grain size (Fig. 4) shows an increase in the K_{IC} as the grain size increases. By studying the variation of fracture energy γ (J/m^2) as a function of the grain size, and by noting that $\gamma = \{(1-\nu)^2/2E\}K_{IC}{}^2$, Simpson[29] links this increase to the development of microcracks. We notice that ceramic A is out of the curve. This alumina has the highest value of hardness and thus a stronger brittleness.

By plotting the toughness curve vs. pore diameter (Fig. 5), we can note the existence of three curves corresponding to three family types: without zirconia (A, B), without CaO (E, H) and the other ceramics. For these three evolutions, toughness decreases as the size of pores increases, this is coherent with the nature and the critical defect size. Let us note that toughness is higher in the case of ceramics containing zirconia, confirming the effect of toughening.[10,11]

3.3. Friction and wear

3.3.1. Friction coefficient

The evolution of the friction coefficient as a function of the number of cycles is shown in Fig. 6. In all cases a progressive increase in the friction coefficient up to a stable value is observed. This evolution is due to microcracking in the surface asperities, which leads to the generation of agglomerated wear debris ("third body"[16,18]). The friction coefficient μ characterizing the faculty of the tribosystem to dissipate energy, then, any storage of energy will be characterized by an increase in μ and conversely.[26] The stabilization of the friction coefficient is a result of an equilibrium situation with a constant quantity of debris continuously formed in the contact. The difference between the studied samples lies in the number of cycles necessary for the stabilization of the friction coefficient (Table 3). It is higher for samples A, E, and G (25 cycles) than for the other samples (between 5 and 12 cycles).

3.3.2. Wear volume

The values of the wear volume obtained for 100 or 400 cycles for a load of 1 daN are summarized in Table 3. As shown in Fig. 7a, for most of alumina materials, after 100 friction cycles, friction tracks observed by SEM, showed the existence of a layer of wear debris (third body). This layer tends to change its aspect, either with stabilization of the third body (B, F) or with significant wear of ceramics (D, H, I). Effectively, after 400 friction cycles, in the case of alumina B, E, F and A, another surface morphology is observable (Fig. 7 b), the comparison with the data of Table 3, gives information about the evolution of degradation. Alumina B and F, which present a strong wear during the first 100 friction cycles, show the weakest wear after 400 cycles. Consequently the third body layer constitutes a screen and protects the sample from wear (Fig. 7b). However, alumina D, H and I continue to wear out because the debris present in the interface, without adhering, are abrasive and increase the wear (Fig. 7b). For alumina G, the presence of debris (Fig. 7b) does not protect the surface of the sample, and we can suppose that their compact state maintains their abrasive capacity, which results in an increase in wear.

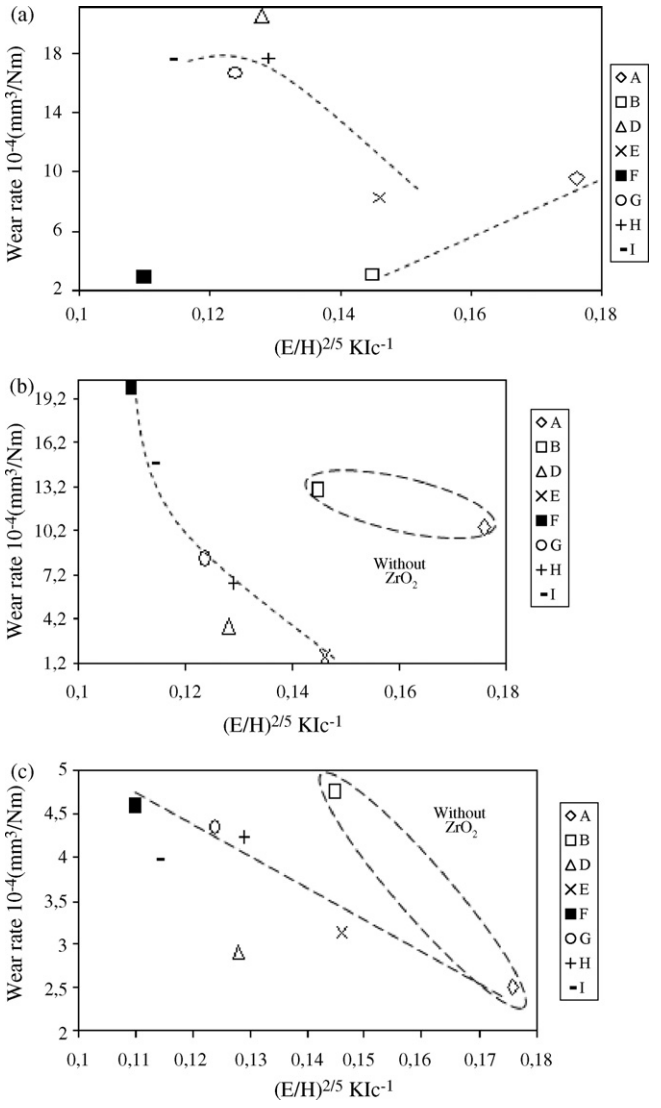

Fig. 8. Application of the mechanical analysis of fractures by indentation, correlation with the wear rates measured in air for: (a) load of 1 daN and 400 cycles, (b) load of 6 daN and 100 cycles and (c) load of 6 daN and 400 cycles.

3.3.3. Correlation between mechanical properties and wear

The Evans's model[32] has been used. It is based on the analysis of fracture by indentation, and predicts the susceptibility of a material to the propagation of cracks around an indentation, linked to the quantity $C^{3/2}\cdot P^{-1}$, proportional to $(E/H)^{2/5}\ K_{IC}{}^{-1}$ (C length of the cracks, P applied load, E Young's modulus, H microhardness and K_{IC} toughness).

Fig. 8 represents the wear rate (mm^3/mN) for a sliding distance of 400 cycles for an applied load of 1 daN (Fig. 8a) and for sliding distances of 100 (Fig. 8b) or 400 cycles (Fig. 8c) respectively for an applied load of 6 daN, as a function of $(E/H)^{2/5}\cdot K_{IC}{}^{-1}$. The wear rate for a strong load (6 daN)

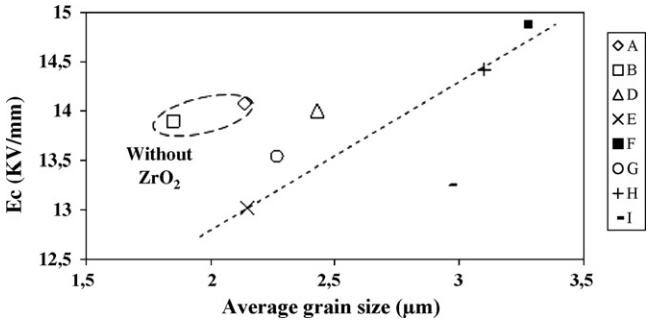

Fig. 9. Evolution of the breakdown strength vs. grains size.

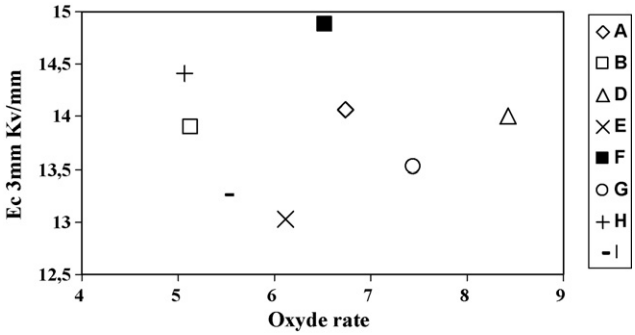

Fig. 10. Evolution of the breakdown strength vs. the total additive content (except zirconia).

decreases (Fig. 8b and c), when $(E/H)^{2/5}\cdot K_{IC}{}^{-1}$ decreases. However, ceramics A and B, without zirconia are outside the curves. This result is comparable with results of Trabelsi et al.[16] which observed that Evans's model only is applicable for ceramics with nearly the same composition. For the low loads (1 daN), the correlation is bad (Fig. 8a).

3.4. Breakdown strength

Table 3 gives the values of breakdown strength and the standard deviations of the studied ceramics. Breakdown strength strongly depends on the microstructure of the alumina. But, as shown recently, the breakdown depends essentially on the nature of the inter-granular phases: glass, anorthite and spinel etc.[33] Those phases control the trapping and/or the diffusion of the electric charges.[25] At room temperature, the breakdown strength is improved when materials are able to stabilize a great amount of electric charges. This behaviour is favoured for materials with microstructures containing many interfaces (i.e. many interfacial phases) in the grain boundaries.[33] The presence of cordierite seem particularly favourable. Ceramics F and H contain cordierite (Table 2) and have, a priori, a high interface number, thus more traps what leads to a high breakdown strength (14.9 and 14.4 kV/mm). In the case of ceramics B, in spite of the high number of interfaces, the nature of inter-granular phases, without cordierite, probably leads to other types of interfaces which decrease breakdown strength (13.9 kV/mm). By comparing these ceramics, it seems to be confirmed that the presence of cordierite in grain boundaries is favourable to the breakdown resistance.

3.4.1. Grain size

We can note that the breakdown strength varies according to the type of addition and of the grain size (Fig. 9). Ceramics A and B, without zirconia, are distinguished from the others with a low grain size and average breakdown strength. The alumina-zirconia materials follow a tendency of increase in rigidity with the grain size, whereas the opposite tendency could be found in the literature for alumina without zirconia.[12,13]

It is possible that zirconia was better distributed on the joints of large grains (F, H), thus increasing the number of sites of trapping of charges. However, it is certain that, in parallel to zirconia addition, the inter-granular phase changes as for the vitreous and crystallized phases taking into account the evolutions in additives (SiO_2, CaO, MgO). Let us recall that the presence of inter-granular crystalline phases leads to traps deeper than those due to a vitreous phase and thus leads to higher breakdown strength at room temperature.[12,13,31]

This is confirmed in Fig. 10, where no relation between the breakdown strength and the total additive percentage (except zirconia) is shown: it is the nature of the secondary phases and not their quantity which influences breakdown strength. This can explain why ceramic I presents a low breakdown strength because of its low content in additive percentage (except zirconia) related to low content in SiO_2 and MgO, but a strong percentage in CaO: its inter-granular phases must be different from those of the other ceramics material which contain zirconia).

3.4.2. Densification

We can note the absence of the influence of the densification beyond 92.5%. However below this value, a fast decrease of E_c and a strong dispersion (Table 3), has been noted for ceramic E, particularly porous (Fig. 11). Thus, the effect of porosity alone is difficult to assess because the effect of the grain boundary is predominant.[12,13]

3.4.3. Analogy between dielectric breakdown and toughness

Except for the ceramics A and B which do not contain zirconia and so have a weak toughness, in case of ceramics E, D, H and F, breakdown strength increases with increasing toughness (Fig. 12), result in agreement with the Fothergill's[34] work. Let

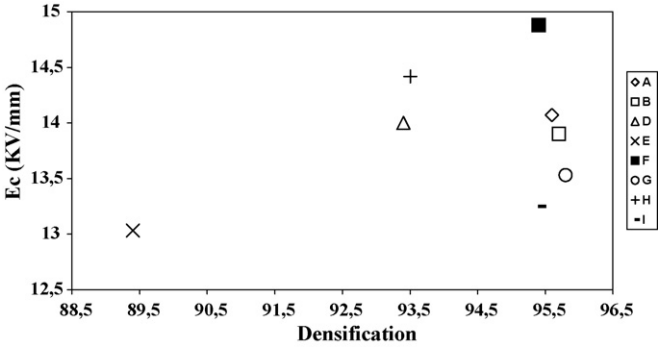

Fig. 11. Evolution of the breakdown strength vs. densification.

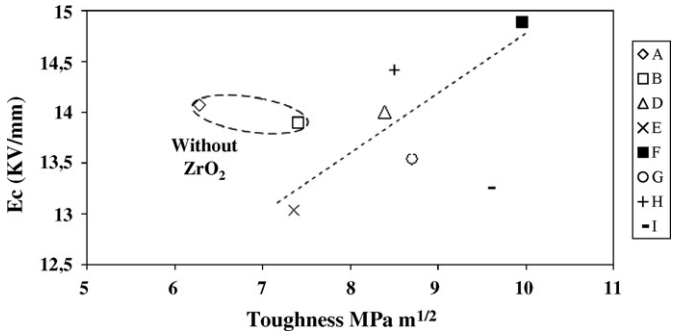

Fig. 12. Variation of the breakdown strength vs. microhardness.

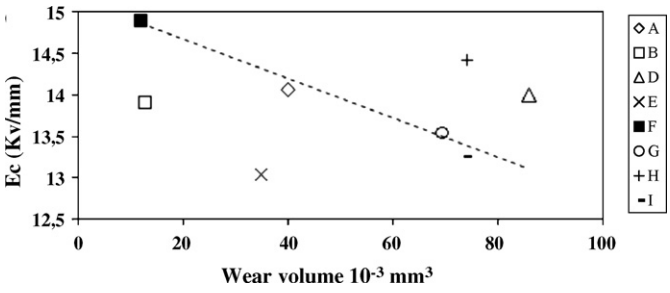

Fig. 14. Evolution of breakdown strength vs. wear volume (V_2) for an applied load of 1 daN, after 400 cycles.

us notice a strong analogy with Fig. 9 (breakdown strength vs. grain size) and Fig. 4 (toughness vs. grains size), the effect of the grain size is thus a significant parameter between breakdown strength and toughness (mechanical property/dielectric property). Ceramic I is characterized by a low breakdown strength and a high toughness, probably due to a favourable inter-granular phase from the mechanical point of view but not from the dielectric point of view.

3.4.4. Analogy between dielectric breakdown and wear

During the first friction cycles (<100 cycles, 1 daN), we notice that wear volume and breakdown strength increase in the same way (Fig. 13). Indeed, strong breakdown strength at room temperature can be related to strong capacity to trap charges at interfaces localized in the grain boundaries. There is thus a strong localization of polarization energy on the grain boundaries which, during relaxation of this energy under friction effect, will release significant energy. This energy can lead to severe wear, which is able to involve a multi-cracking of the alumina grains which, with the secondary phases, can create a fine and protective third body. For a softer relaxation (low breakdown strength), the particles of wear will be larger and the third body less stable. This is typical of ceramics F: characterized by a strong breakdown strength associated with a strong initial wear. The third body formed (Fig. 7) will then lead to the weakest wear after 400 cycles. Ceramic I (low breakdown strength) and especially ceramic D (strong porosity) do not follow the general tendency for 100 cycles: in fact for this distance, these materials are already in severe wear mode, controlled mainly by the nature of the formed third body. This can be seen for all ceramics at 400 cycles (Fig. 14) where it is difficult to establish a relationship between breakdown strength and wear volume, even if the general tendency leads to the correspondence: strong breakdown strength involves weak wear. This can be explained by a protection of the alumina matrix by a stable and adhering third body: the relaxation of polarization energy, therefore wear, occurs as much less in the matrix as its breakdown strength is high.

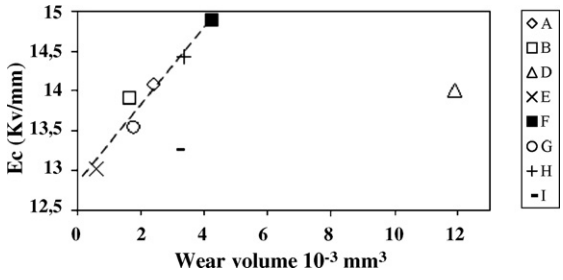

Fig. 13. Variation of breakdown strength vs. toughness.

In conclusion: the electrostatic phenomenon strongly influences the first steps of wear. The trapping of electric charges at grain boundaries lead to brutal relaxation of polarization energy being able to affect the microstructure of the third body: it can be formed by fine debris in the case of strong trapping (high breakdown strength), and by larger debris in the case of weak trapping (low breakdown strength). Another element which affects the third body, will be related to the nature of the secondary phases: this can explain weak wear at 400 cycles of ceramics B and F, which have nearly the same additives content (except zirconia).

4. Conclusion

In this study, alumina ceramics were elaborated using the same process and starting from the same products. Several compositions lead to vary not only microstructural parameters (grain size, porosity. . .) but also the nature of the inter-granular phases. Moreover, the addition of the same zirconia content permits to see its good influence on not only mechanical but also dielectric properties.

Two microstructural parameters especially significant were put forward: the average grain size and the nature of secondary phases. It is obvious that these two parameters are not independent as well from the mechanical point of view as electrical point of view. Porosity and densification have a weak influence beyond 92% of densification.

On the other hand, the increase in the average grain size leads to an increase in hardness, toughness and breakdown strength. The latter characteristic is much related to the nature of the inter-granular phases. One can suppose that the parameter most relevant, but difficult to identify, would be the composition of the secondary phases.

Wear is a complex phenomenon, able to unite together dielectric and mechanical aspects. At the first steps of wear (low load, short time), the dielectric phenomena seem to have a significant role on the fracturing of alumina grains. If fracturing is violent (corresponding to high breakdown strength), the debris (fractured alumina grains and released inter-granular phases) can form a finely agglomerated third body. The latter will be able to

protect the substrates. At this stage, the mechanical parameters (hardness, toughness or Evans's factor) are not relevant.

For more severe conditions (time, load), the nature of the third body (formed during the preceding step) plays an essential role: finely agglomerated and adherent, it ensures the bearing screen which avoids the wear of bulk alumina. A strong breakdown strength will avoid the dielectric relaxation of alumina and thus its wear.

However, this study highlighted the correspondence "breakdown strength–toughness". It is not useless to note that toughness, measured here by indentation, comprises problems of indenter-alumina friction associated with creation of dislocations[22] and then cracking just like the observations made in dielectric breakdown.[23]

References

1. Virkar, A. V. and Gordon, R. S., Fracture properties of polycrystalline lithia-stabilized alumina. *J. Am. Ceram Soc.*, 1977, **60**(1–2), 58–61.
2. Rice, R. W., Freiman, S. W. and Becher, P. F., Grain size dependence of fracture energy in ceramics. *J. Am. Ceram. Soc.*, 1981, **64**, 345–350.
3. Simpson, L. A., Ritchie, I. G. and Lloyd, D. J., Cause of the discrepancy resulting from testing methods in the relation of grain size and fracture energy in Al_2O_3. *J. Am. Ceram. Soc.*, 1975, **58**(11–12), 537–538.
4. Noone, M. J. and Mehan, R. L., *Fracture Mechanics of Ceramics*, *vol. 1*, ed. R. C. Bradt, D. P. H. Hasselman and F. F. Lange. Plenum, New York, 1973.
5. Simpson, L. A., Effect of microstructure on measurement of grain size dependence of fracture energy in Al_2O_3. *J. Am. Ceram. Soc.*, 1973, **56**(1), 7–11.
6. Tani, T., Miyamoto, Y., Koisumi, M. and Shimada, M., Grain size dependence of Vickers microhardness and fracture toughness in Al_2O_3 and Y_2O_3. *Ceram. Int.*, 1986, **12**, 33–37.
7. Page, T. F. and Sargent, P. M., *Proc. Br. Ceram. Soc.*, 1978, **26**, 209–224.
8. Knudsen, F. P., Dependence of the mechanical properties of brittle polycrystalline specimens on porosity and grain size. *J. Am. Ceram. Soc.*, 1959, **42**(8), 376–387.
9. Passmore, E. M., Spriggs, R. M. and Vasilos, T., Strength-grain size-porosity relations in alumina. *J. Am. Ceram. Soc.*, 1973, **48**(1), 1–7.
10. Claussen, N., Stress-induced transformation of tetragonal Zr_2O_2 particles. *J. Am. Ceram. Soc.*, 1978, **61**(1–2), 85–86.
11. Evans, A. G. and Heuer, A. H., Transformation toughening in ceramics: martensitic transformation in crack-tip stress. *J. Am. Ceram. Soc.*, 1980, **63**(5–6), 241–248.
12. Liebault, J., Comportement d'alumines face à l'injection des charges. Relation microstructure-claquage diélectrique-mesure de charge d'espace. Thèse Ecole Nationale Supérieure des Mines de St Etienne, N°206 TD, 1999.
13. Liebault, J., Vallayer, J., Goeuriot, D., Tréheux, D. and Thevenot, F., How the trapping of charges can explain the dielectric breakdown performance of alumina ceramics. *J. Eur. Ceram. Soc.*, 2001, **21**, 389–397.
14. Morse, C. T. and Hill, G. J., The electric strength of alumina: the effect of porosity. *Proc. Br. Ceram. Soc.*, 1970, **18**, 23.
15. Beaudet, S., Bernier, J. C. and Autissier, D., Doping elements influence on microstructural and dielectric properties of alpha alumina. *Key Eng. Mater.*, 1997, **132–136**, 1179.
16. Trabelsi, R., Tréheux, D., Orange, G., Fantozzi, G., Homerin, P. and Thévenot, F., Relationships between mechanical properties and wear resistance of alumina–zirconia ceramic composite. *J. Am. Soc. Lubrication Eng. Tribol. Trans.*, 1989, **32**, 77–84.
17. Berriche, Y., Vallayer, J., Trabelsi, R. and Treheux, D., Severe wear of Al_2O_3–AlON ceramic composite. *J. Eur. Ceram. Soc.*, 2003, **20**, 1829–1836.
18. Kim, S., Kato, K., Hokkirigawa, K. and Abe, H., Wear mechanism of ceramic materials in dry rolling friction. *J. Tribol.*, 1986, **108**, 522.
19. ZumGahr, K. H. and Bundshuh, W., Effect of grain size and sliding wear of oxide ceramics. *Wear*, 1993, 162–164.
20. Mukhopadhyay, A. K. and Yiu–Wing, Mai, Grain size effect on abrasive wear mechanisms in alumina ceramics. *Wear*, 1993, **162-164**, 258–268.
21. W.U., C. and Rice, R. Z., Porosity dependence of wear and other mechanical properties of fine grain Al_2O_3 and B_4C. *Ceram. Eng. Sci. Proc.*, 1985, **6**(7–8), 977–994.
22. Hockey, B. J., Plastic deformation of aluminium oxide by indentation and abrasion. *J. Am. Ceram. Soc.*, 1971, **54**(5), 223.
23. Zhong, X.-F., Shen, C.-F., Song Liu, Y. and Zhang, C.-R., Model for radiation induced degradation of αAl_2O_3 crystals. *Phys. Rev. B*, 1996, **54**(1), 139–143.
24. Le Gressus, C. and Blaise, G., Breakdown phenomena related to trapping/detrapping processes in wide band-gap insulators. *IEEE Trans. Electr. Insul.*, 1992, **27**, 472–481.
25. Touzin, M., Goeuriot, D., Fitting, H. J., Guerret-Piécourt, C., Juvé, D. and Tréheux, D., Relationships between dielectric breakdown resistance and charge transport in alumina materials-Effects of the microstructure. *J. Eur. Ceram. Soc.*, 2007, **27**, 1193–1197.
26. Fayeulle, S., Berroug, H., Hamazaoui, B., Tréheux, D. and Le Gressus, C., Role of dielectric properties in the tribological behaviour of insulators. *Wear*, 1993, **162–164**, 906–912.
27. Tréheux, D., Bigarré, J. and Fayeulle, S., Dielectric aspects of the ceramic tribology. In *9th Cimtec World Ceramics Congress. Ceramics getting into 2000s. Part A. Techna Srl*, ed. P. Vincenzini, 1999, pp. 563–574.
28. Guerret-Piécourt, C., Vallayer, J. and Tréheux, D., Limitation induced by electrical charges effects on micromechanisms. *Wear*, 2003, **254**, 950–958.
29. Barceinas-Sanchez, J. D. O. and Rainforth, W. M., On the role of plastic deformation during the mild wear of alumina. *Acta Mater.*, 1998, **46**(18), 6474–6483.
30. Liang, K. M., Orange, G. and Fantozzi, G., Evaluation by indentation of fracture toughness of ceramic materials. *J. Mater. Sci.*, 1990, **25**, 207–214.
31. Simpson, L. A., Ritchie, I. G. and Lloyd, D. J., *J. Am. Ceram. Soc.*, 1975, **58**(11–12), 537–538.
32. Evans, A. G., The science of ceramic machining and surface finishing. In *National Bureau of Standards Special Publication 562*, ed. B. J. Hockey and R. W. Rice. US.Government Printing office, Washington D.C. P1, 1979.
33. Touzin, M. and Goeuriot D., Alumina based ceramics for high-voltage insulation—part I: influence of elaboration parameters on dielectric breakdown resistance, J. Eur. Ceram. Soc., 2009, submitted for publication.
34. Fothergill, J. C., Filamentary electromechanical breakdown. *IEEE Trans. Electr. Insul.*, 1991, **26**(6), 1124–1129.